TABLE 1 Carbon isotope values of SiC and diamonds from Fuxian

Mineral	Number of crystals	Weight (mg)	Description	$\delta^{13}C$ (‰)*
α-SiC	Numerous	20	blue	−24.0
Diamond	11	12	white, flawless	−2.9
Diamond	19	16	white, deeply etched	−4.5
Diamond	11	10	white, with deformation lamellae	−4.4
Diamond	1	17	pale yellow, flawless	−3.8
Diamond	4	23	pale yellow, flawless	−4.8

Carbon extraction technique: Samples were heated at 1,000 °C for 45 min in circulating O_2 at 1 atm. The combustion tube contained Pt and Cu oxides to oxidize any CO produced during the experiment. 97% of the SiC combusted during the first 5 min, and the remainder combusted within the next 15 min. Yields were better than 99%.

* $\delta^{13}C = [(^{13}C/^{12}C)_{sample}/(^{13}C/^{12}C)_{standard}] - 1$, where the standard was Pee Dee belemnite (PDB).

result of an incomplete displacive transformation, or a quenched high-quartz structure. Crystallization of SiO_2 as quartz instead of coesite indicates a maximum pressure of <20–28 kbar at 1,000–1,200 °C, estimated using equilibrium lines of high quartz/low quartz[17] and quartz/coesite[18] transitions. Under the above pressure and temperature conditions, the stable polymorph of SiO_2 is high quartz, and not tridymite or cristobalite which are stable only at pressures below 10 kbar[19]. Thus, β-SiC must have crystallized in a more oxidizing environment at a depth of 60–90 km where the temperature may be ~1,000 °C, the minimum temperature at which SiC can be synthesized in the laboratory[16].

Results of our carbon isotope analyses are presented in Table 1. The $\delta^{13}C$ values of diamond samples fall in the range, −2.9‰ to −4.8‰ (average = −4.1‰), whereas the value for α-SiC is −24.0‰, indicating a strong ^{12}C enrichment in SiC, ~20‰. Large differences in isotopic compositions have also been observed in diamonds from worldwide localities[20–22]. Hypotheses proposed to account for such isotope heterogeneities include multiple sources of mantle carbon[23], introduction of organic carbon by subduction[24], and extreme fractionation by degassing of the mantle[25], all suggestive of disequilibrium growth of diamonds. As no evidence from diamond research is presently available to justify these hypotheses, we shall discuss an alternative.

Isotopically zoned but non-coated diamonds[23,26] show variations in ^{13}C from core to rim of only about 4‰. We suggest that the 20‰ fractionation observed between SiC and diamond is due to a distillation process: preferential uptake of ^{13}C during the growth of SiC enriched the carbon reservoir, in which the diamond later grew, in ^{12}C. Evidence that the SiC was formed first is provided by the presence of SiC inclusions in diamonds from Fuxian[13]. To explain the preferential uptake of ^{13}C by SiC, we examined the thermodynamic properties (1 atm) of diamond[27] and 6H SiC[28] and found that SiC has much higher enthalpy and entropy than diamond. Deines[29] noted that in an isotope exchange reaction, the solid of lower heat capacity can be correlated with higher vibrational frequency and a stronger tendency to incorporate the heavy isotope. This suggests that SiC should be enriched in ^{13}C and diamond in ^{12}C, as we observe.

In studies of iron meteorites[30,31], systematic ^{12}C enrichment in graphite and ^{12}C depletion in cohenite (iron carbide), in 12‰ fractionation at ~600 °C was observed, and the fractionation was expected to increase with increasing temperature. The ^{13}C-^{12}C systematics observed in our SiC-diamond system is completely analogous. Our isotope data imply that the carbon reservoir in the mantle beneath Fuxian has a $\delta^{13}C$ value between −24‰ and −4‰, and is probably much lower than −5‰, a value derived from isotope analysis of natural diamonds. A more precise estimate would require a knowledge of all fractionation processes and the number of carbon-bearing phases participating in the isotope exchange reaction. □

Received 26 October 1989; accepted 25 May 1990.

3. Gurney, J. J. in *Kimberlites and Related Rocks* Vol. 2 (eds Ross, J. *et al*), 935–965 (Blackwell, Carlton, 1989).
2. Moissan, H. *C.r. hebd. Séanc. Acad. Sci., Paris* **139,** 773–780 (1904).
3. Mason, B. *Am. Miner.* **52,** 307–325 (1967).
4. Bobrievich, A. P., Kalyuzhuyi, V. A. & Smirnov, G. I. *Dokl. Akad. Nauk SSSR* **115,** 1189–1192 (1957).
5. Bauer, J., Fiala, J. & Hřichová, R. *Am. Miner.* **48,** 620–634 (1963).
6. Marshintsev, V. K., Shchelchkova, S. G., Zol'nikov, G. V. & Voskresenskaya, V. B. *Geol. Geofiz. Novosib.* **12,** 22–31 (1967).
7. Regis, A. J. & Sand, L. B. *Geol. Soc. Am. Bull.* **69,** 1633 (1958).
8. Marshintsev, V. K., Zayakina, N. V. & Leskova, N. V. *Dokl. Akad. Nauk SSSR* **262,** 204–206 (1982).
9. Lyakhovich, V. V. *Izv. Acad. Nauk SSSR, Ser. Geol.* **4,** 63–74 (1979).
10. Milton, C. & Vitaliano, D. B. *Geol. Soc. Am. Abstr. Prog.* **17,** 665 (1985).
11. Gauthier, J. P. *J. Microsc.* **119,** 189–197 (1980).
12. Woermann, E., Knecht, B., Rosenhauer, M. & Ulmer, G. C. *Proc. 2nd Int. Conf. Kimberlites* Abstr. (1977).
13. Leung, I. S. *Am. Miner.* (in the press).
14. Woermann, E. & Rosenhauer, M. *Fortschr. Miner.* **63,** 263–349 (1985).
15. Harris, P. G. in *Kimberlite Occurrence and Origin* (eds Glover, J. E. & Harris, P. G.) 125–142 (Univ. Western Australia, Nedlands, 1985).
16. Knippenberg, W. F. *Philips Res. Rep.* **18,** 161–274 (1963).
17. Cohen, L. H. & Klement, W. *J. geophys. Res.* **72,** 4245–4251 (1967).
18. Böhler, R. & Arndt, J. *Contr. Miner. Petrol.* **48,** 149–152 (1974).
19. Zoltai, T. & Stout, J. H. *Mineralogy: Concepts and Principles* (Burgess, Minneapolis, 1984).
20. Koval'skii, V. V. & Cherskii, N. V. *Ind. Diam. Rev.* **33,** 54–56 (1973).
21. Galimov, E. M. *Geokhimiya* **8,** 1091–1118 (1984).
22. Deines, P., Harris, J. W. & Gurney, J. J. *Geochim. cosmochim. Acta* **51,** 1227–1243 (1987).
23. Boyd, S. R. *et al. Earth planet. Sci. Lett.* **86,** 341–353 (1987).
24. Milledge, H. J. *et al. Nature* **303,** 791–792 (1983).
25. Javoy, M., Pineau, F. & Iijima, I. *Contr. Miner. Petrol.* **67,** 35–39 (1978).
26. Swart, P. K., Pillinger, C. T., Milledge, H. J. & Seal, M. *Nature* **303,** 793–795 (1983).
27. Berman, R. in *Physical Properties of Diamond* (ed. Berman, R.) 371–393 (Clarendon, Oxford, 1965).
28. Humphrey, G. L., Todd, S. S., Coughlin, J. P. & King, E. G. *Bur. Mines Rept. Invest. 4888* (U.S. Dept. inter., Pittsburgh, 1952).
29. Deines, P. & Wickman, F. E. *Geochim. cosmochim. Acta* **39,** 547–557 (1975).
30. Deines, P. & Wickman, F. E. *Geochim. cosmochim. Acta* **37,** 1259–1319 (1973).
31. Broecker, W. S. & Oversby, V. M. *Chemical Equilibria in the Earth* (McGraw-Hill, New York, 1971).

ACKNOWLEDGEMENTS. We thank P. Dienes and G. Ulmer for discussions. This work was supported in part by the Research Corporation.

Rb–Sr dating of sphalerites from Tennessee and the genesis of Mississippi Valley type ore deposits

Shun'ichi Nakai, Alex N. Halliday, Stephen E. Kesler & Henry D. Jones

Department of Geological Sciences, University of Michigan, Ann Arbor, Michigan 48109-1063, USA

MISSISSIPPI Valley type (MVT) ore deposits commonly consist of some combination of lead, zinc and iron sulphides accompanied by barite, fluorite, dolomite and calcite. They are thought to form by fluid expulsion from sedimentary successions[1–3], but their exact origin has remained controversial because of the scarcity of reliable geochronological data. In a recent and widely quoted model the MVT deposits of the central and eastern United States formed as a result of large-scale lateral fluid flow driven by the tectonic squeezing of sedimentary successions during the late Palaeozoic Alleghenian orogeny (330–250 Myr)[4]. Here we report the first direct Rb–Sr dating of sphalerites from an MVT deposit and propose this as a useful geochronological technique for sulphide mineralization with poor age control. Rb–Sr data for sphalerites from Coy mine, East Tennessee, define an isochron age of 377 ± 29 Myr, ruling out any genetic connection with the Alleghenian orogeny. Instead, MVT mineralization in the eastern United States was apparently generated from fluids expelled during thrusting associated with the older Acadian orogeny (380–350 Myr).

The difficulty in isotope dating the MVT deposits is due to

TABLE 1 Rb–Sr data for sphalerites and their fluid inclusions

Sample number		Rb (p.p.m.)	Sr (p.p.m.)	$^{87}Rb/^{86}Sr$	$^{87}Sr/^{86}Sr$	Apparent sphalerite-fluid age (Myr)*
C5L	r	0.06686	0.2805	0.6868	0.714635 (69)†	358 ± 21
	l	63.05	3,393	0.05349	0.711404 (85)	
C14I	r	0.2943	1.462	0.5796	0.713633 (19)	306 ± 8
	l	142.1	5,539	0.07387	0.711428 (13)	
C14II	r	0.3364	0.8808	1.101	0.716706 (22)	373 ± 8
	l	150.4	9,984	0.04337	0.711096 (47)	
C15	r	0.2290	1.056	0.6247	0.712408 (20)	150 ± 9
	l	371.1	979.8	0.1090	0.711308 (37)	
C16D	r	0.1707	1.386	0.3549	0.712483 (16)	333 ± 11
	l	47.16	2,403	0.05652	0.711070 (18)	
C16L	r	0.4755	1.858	0.7374	0.714931 (20)	441 ± 9
	l	73.58	1,697	0.1240	0.711079 (21)	
C18	r	0.05042	0.6601	0.2200	0.711761 (16)	233 ± 24
	l	62.10	2,085	0.08579	0.711316 (50)	
C44	r	0.2631	0.4134	1.835	0.720396 (23)	

Rb and Sr were separated using standard ion-exchange procedures[26], and their concentrations measured by isotope dilution using a mixed $^{87}Rb/^{84}Sr$ spike. In the first column, r and l denote residue and leachate, respectively. Rb and Sr concentrations of fluid inclusions were calculated assuming that the weight fraction of fluid inclusions in the sphalerites was 300 p.p.m. (see text). Isotope measurements were performed using a VG Sector mass spectrometer. During this study, an average $^{87}Sr/^{86}Sr$ value of NBS 987 Sr standard was 0.710256 (5) (where the number in parentheses indicates the 2σ uncertainty). The decay constant $\lambda\ ^{87}Rb = 1.42 \times 10^{-11}\ yr^{-1}$ was used for the age calculation.

* Uncertainty calculated by combining run precision on Sr isotopic composition with an uncertainty of 1% (2σ) on the $^{87}Rb/^{86}Sr$ ratio.

† 2σ uncertainty.

the lack of suitable minerals with high or variable parent/daughter ratios. This has led to indirect attempts to determine their age. One approach has been to date apparent resetting from hydrothermal fluids. For example, the Rb–Sr age of glauconites has been used to estimate the age of mineralization in the Viburnum Trend[5] (a 75-km-long belt of MVT mineralization in Missouri), based on the assumption that the formation of the MVT deposit was the last process to affect the isotope system in the glauconites. A second approach is to use model ages. For example, Halliday *et al.*[6] used the large fractionation in Sm/Nd ratios in fluorites from the North Pennine Orefield to place constraints on the timing of mineralization. Similarly, Kesler *et al.*[7] estimated that the mineralization in the Mascot-Jefferson City district in East Tennessee was younger than 395 Myr using a crude basin-evolution model. As with model lead ages, the interpretations are critically dependent on the inferred isotope evolution of the source of the components, which is seldom well defined. There have been very few attempts to date ore constituents directly—one notable exception was that of Lange *et al.*[8] who attempted to date galenas from the Viburnum mine in southeast Missouri using the Rb–Sr method. In addition, Medford *et al.*[9] reported Sr isotope data for sulphide and carbonate minerals from Pine Point mine, Canada, and noted that sphalerite can have a high Rb/Sr ratio which could facilitate its use in isotope dating.

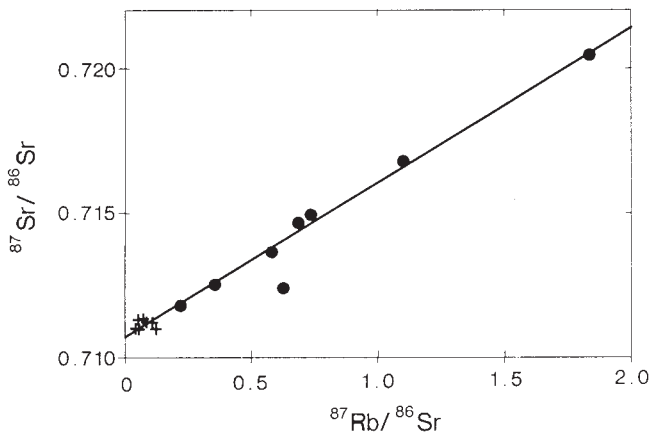

FIG. 1 Rb–Sr isochron of sphalerites from Coy mine. Circles and crosses denote residues and leachates, respectively. Eliminating a point for C15 (see text), the isochron yields an age of 377 ± 29 Myr (mean square of weighted deviates is 62.6).

The deposits in the Mascot-Jefferson City district, East Tennessee, are hosted by the Lower Ordovician Knox group. The top of the Knox group is marked by an extensive Middle Ordovician unconformity, and the ores below occur in collapse breccias formed by karstification[10]. Palaeomagnetic measurements[11] and K–Ar age determinations on clays and K-feldspars in this district[12,13] have been interpreted as indicating large-scale fluid migration in the late Palaeozoic, which led to the view that the Appalachian MVT deposits in East Tennessee were formed by massive movements of fluid expelled from sedimentary basins during the Alleghenian orogeny (330–250 Myr)[4].

Rb–Sr data for eight leached samples of sphalerite, together with seven of their (fluid inclusion) leachates are presented in Table 1 and Fig. 1. For each analysis ~100 mg of hand-picked, washed sphalerite was crushed in deionized water and leached with the water to remove the fluid-inclusion contents. The absolute concentrations of Rb and Sr in the fluid inclusions can only be estimated because of the inability to measure accurately the mass of the inclusions. Haynes *et al.*[14] have reported that gas chromatographic analyses of fluid inclusions in sphalerites from Mascot-Jefferson City district yielded between 3 and 49 μmol per g H_2O (average 13.5 μmol per g) and that the salinities of the fluid inclusions were ~20%. From these data, we estimate that the weight fraction of fluid inclusions in the sphalerites averaged ~300 p.p.m. Rb and Sr concentrations in the fluid inclusions shown in Table 1 were calculated using this value, and are estimated to be accurate to within an order of magnitude. The Rb/Sr ratios, however, are accurate to better than 1%. After removal of the fluid inclusions, the sphalerites were dissolved in hot 6M hydrochloric and concentrated nitric acid (9:1). The sphalerites have low Sr concentrations (<2 p.p.m.), but variable $^{87}Rb/^{86}Sr$ ratios (0.3–2.0).

The isotope data are plotted on a conventional isochron diagram in Fig. 1 and, with the exception of C15, all the sphalerites show a clear correlation between $^{87}Rb/^{86}Sr$ ratios and $^{87}Sr/^{86}Sr$ ratios. The scatter observed probably reflects heterogeneity in the initial Sr isotopic compositions of the sphalerites—such isotope variability for mineralizing solutions is well documented for MVT deposits[8,15]. In addition, the introduction of secondary fluids and the deformation of the ore

constituents may also have disturbed the Rb–Sr system. Sample C15 was notably more deformed than the other samples. Ignoring this point, the data for the sphalerites define an apparent isochron age of 377 ± 29 Myr (2σ) with an initial $^{87}Sr/^{86}Sr$ ratio of 0.7107(3) (2σ uncertainty).

The leachates (fluid inclusions) have lower $^{87}Rb/^{86}Sr$ ratios (<0.1) than the sphalerites and cluster around the lower end of the isochron in Fig. 1. Calculated apparent Rb–Sr ages for leach–sphalerite pairs are shown in Table 1. The ages obtained are extremely variable, ranging from 150 to 440 Myr. These data indicate that in the relatively large samples required for this study, several types of inclusion fluids (known to exist) were sampled, including secondary fluids not directly related to sphalerite precipitation.

Figure 2 shows a chondrite-normalized rare-earth element (REE) pattern for sample C16D (after removal of the inclusion fluids). As far as we are aware, high-precision REE analyses of sphalerites have not been previously reported. Although the concentrations are low, the pattern is strikingly similar to that of average shales[16]. If the REEs in the sphalerite were derived from the hydrothermal fluids no major fractionation can have occurred during mineralization.

The exact location of the Rb, Sr and REEs in the sphalerites is uncertain. The Rb/Sr ratio is much too high for the components to be derived from carbonate, fluorite or barite inclusions. From the Rb/Sr ratio (0.12) and Sr/Nd ratio (90) of C16D, clay or feldspar are more likely host phases. Scanning electron microscopy (SEM) of the hand-picked sphalerites did not reveal any silicate phases on the micrometre scale except quartz and very rare feldspar on the surface of some of the grains. The K-feldspar seems to predate sphalerite in all samples that we have examined. The sphalerite and feldspar are distributed together in silica-rich alteration zones[13] which are thought to be coeval with mineralization[17]. Our SEM measurements indicate that feldspar inclusions probably constitute ≪0.1% of the hand-picked sphalerite, but at least 0.1% is required to explain the Rb and Sr concentrations of C16D. If feldspar is the host of the REEs, the lack of fractionation of Eu relative to a typical crustal pattern (Fig. 2) would require that it grew under non-reducing conditions. We conclude that it is highly unlikely that the Rb–Sr data reflect a dolomite, barite, fluorite or clay component. The Rb, Sr and REEs are most likely hosted in the sphalerite itself or in K-feldspar. These phases are probably cogenetic, therefore the Rb–Sr data should define the age of sphalerite mineralization. If the Rb, Sr and REEs are not held in inclusions, but were sequestered from hydrothermal fluids in minute amounts by the sphalerite, it is not clear how the range in Rb/Sr could have been generated. One possibility is that the composition of the ore fluid evolved with deposition of gangue minerals as a result of different bulk partition coefficients for Rb and Sr. Another possibility is that the variations reflect incomplete mixing of fluids. Both of these seem unlikely because the range of Rb/Sr in the fluid-inclusion contents analysed is relatively restricted (Table 1).

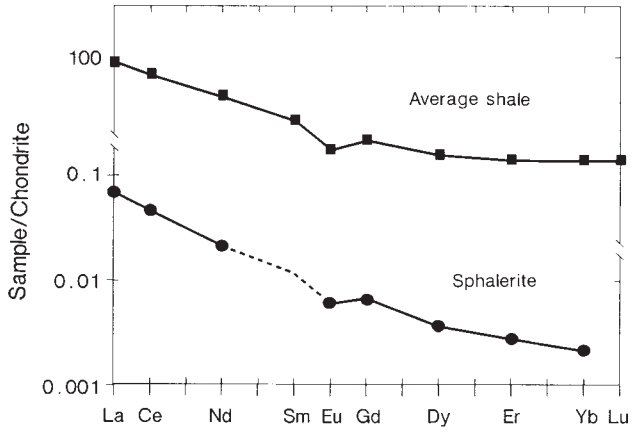

FIG. 2 Chondrite-normalized pattern of a sphalerite, C16D and North American Shale Composite (NASC). The REE abundances in the Leedey chondrite[27] are used to normalize the values. The point for Sm was estimated by interpolating points for Nd and Gd. The pattern of the sphalerite is similar to that of typical crustal material, NASC.

The geologically reasonable isochron age implies that the range in initial Sr isotopic composition in the ore fluids must have been relatively small. Kesler *et al.*[7] and Kessen *et al.*[18] reported Sr isotope data for MVT deposits in East Tennessee and showed that the gangue minerals that precipitated from the early dolomite-forming fluids had similar Sr isotopic composition to the host carbonates ($^{87}Sr/^{86}Sr = 0.7090–0.7092$)[7] whereas $^{87}Sr/^{86}Sr$ ratios for later gangue minerals increased with time up to 0.7122 for paragenetically late calcite. The initial $^{87}Sr/^{86}Sr$ ratio obtained for sphalerites from the isochron intercept in this study (0.7107) is consistent with this trend, being intermediate between the Sr isotopic ratio for pre-ore and post-ore dolomites. Therefore the isotope data are consistent with the idea that the Sr in the sphalerite was sequestered from the ore fluids themselves rather than inherited from unrelated older material in the ore. Furthermore the combined data indicate a relatively small range in Sr isotopic composition of the ore-forming fluids at the time of mineralization.

Our data indicate that mineralization predated the Alleghenian orogeny (330–250 Myr) by ~50 Myr and are therefore inconsistent with the hypothesis that basinal brines tectonically expelled during that event played an important part in ore genesis. Furthermore the alkali feldspar intergrown with sphalerite in these deposits cannot have grown during Alleghenian fluid movements as argued by Hearn *et al.*[13]. Although it is generally considered that the thermal effects of the Acadian orogeny (380–350 Myr) were restricted to areas further east than this district[19], it has been shown that there was major thrusting immediately to the southeast of the district at this time[20]. It seems therefore that uplift and deformation in early Devonian resulted in fluid expulsion and the formation of MVT mineralization to the west. MVT deposits located along the Appalachian mountains from Georgia to Newfoundland have many features in common, such as high Zn/(Zn+Pb) ratios and relatively homogeneous Pb and stable isotopic compositions. Among the Appalachian MVT deposits, the mineralization in the St George Group in Newfoundland is similar in stratigraphic setting to that in East Tennessee[10]. $^{40}Ar–^{39}Ar$ ages of alkali feldspar from MVT ore deposits in western Newfoundland were reported by Hall *et al.*[21]. They concluded that the alkali feldspars were subjected to thermal events at 370–350 Myr and 210 Myr and interpreted the older event as the time of sphalerite mineralization[21]. These data are consistent with the suggestion that Appalachian MVT mineralization was related on a regional scale to the Acadian orogeny.

Oilfield brines are often considered to be suitable ore-forming solutions for MVT deposits[22]. They can have high $^{87}Sr/^{86}Sr$ ratios owing to interactions with silicate minerals in sedimentary successions. The ratios for several oilfield brines range between 0.709 and 0.735[23,24] and our initial Sr isotopic ratio for the sphalerites and the fluid inclusions falls in this range. Furthermore, Chaudhuri *et al.*[25] have reported Rb/Sr ratios for oilfield brines from Kansas of ~0.02, similar to the ratios found in the fluid inclusions from East Tennessee. Our data are therefore consistent with basin-brine-expulsion models for the fluids that formed both the MVT deposit and the fluid inclusions. □

Received 5 March; accepted 23 May 1990.

1. White, D. E. *Econ. Geol.* **63,** 301–335 (1968).
2. Ohle, E. L. *Econ. Geol.* **75,** 161–172 (1980).
3. Sverjensky, D. A. *A. Rev. Earth planet Sci.* **14,** 177–199 (1986).

4. Oliver, J. *Geology* **14,** 99–102 (1986).
5. Stein, H. J. & Kish, S. A. *Econ Geol.* **80,** 739–753 (1985).
6. Halliday, A. N., Shepherd, T. J., Dickin, A. P. & Chesley, J. T. *Nature* **344,** 54–56 (1990).
7. Kesler, S. E., Jones, L. M. & Ruiz, J. *Geol. Soc. Am. Bull.* **100,** 1300–1307 (1988).
8. Lange, S., Chaudhuri, S. & Clauer, N. *Econ. Geol.* **78,** 1225–1261 (1983).
9. Medford, G. A., Maxwell, R. J. & Armstrong, R. L. *Econ. Geol.* **78,** 1375–1378 (1983).
10. Hoagland, A. D. in: *Handbook of Stratabound and Stratiform Ore Deposits.* Vol. 6 (ed. Wolfe, K. H.) 495–534 (Elsevier, Amsterdam, 1976).
11. Bachtadse, V., Van der Voo, R., Haynes, F. M. & Kesler, S. E. *J. geophys. Res.* **92,** 14165–14176 (1987).
12. Elliott, W. C. & Aronson, J. L. *Geology* **15,** 735–739 (1987).
13. Hearn, P. P. Jr, Sutter, J. F. & Belkin, H. E. *Geochim. cosmochim. Acta* **51,** 1323–1334 (1987).
14. Haynes, F. M., Beane, R. E. & Kesler, S. E. *Am. J. Sci.* **289,** 994–1038 (1989).
15. Hart, S. R., Shimizu, N. & Sverjensky, D. A. *Econ. Geol.* **76,** 1873–1878 (1981).
16. Goldstein, S. J. & Jacobsen, S. B. *Earth planet. Sci. Lett.* **94,** 35–47 (1989).
17. McCormick, J. E., Evans, L. L., Palmer, R. A. & Rasnick, F. D. *Econ. Geol.* **66,** 757–762 (1971).
18. Kessen, K. M., Woodruff, M. S. & Grant, N. K. *Econ. Geol.* **76,** 913–920 (1981).
19. Glover, L. III, Speer, J. A., Russell, G. S. & Farrar, S. *Lithos* **16,** 223–245 (1983).
20. Hatcher, R. D. Jr & Odom, A. L. *J. geol. Soc. Lond.* **137,** 321–327 (1980).
21. Hall, C. M., York, D., Saunders, C. M. & Strong, D. F. *Proc. Int. Geol. Congr.* **2,** 10–11 (1989).
22. Sverjensky, D. A. *Econ. Geol.* **79,** 23–37 (1984).
23. Chaudhuri, S. *Geochim. cosmochim. Acta* **42,** 329–331 (1978).
24. Sunwall, M. T. & Pushkar, P. *Chem. Geol.* **24,** 189–197 (1979).
25. Chaudhuri, S., Broedel, V. & Clauer, N. *Geochim. cosmochim. Acta* **51,** 45–53 (1987).
26. Halliday, A. N., Metz, J. M., Dempster, T. J. & Mahood, G. A. *Earth planet. Sci. Lett.* **94,** 274–290 (1989).
27. Masuda, A., Nakamura, N. & Tanaka, T. *Geochim. cosmochim. Acta* **37,** 239–248 (1973).

ACKNOWLEDGEMENTS. We thank R. Keller and M. Johnson for technical assistance. This work was supported by the NSF, the University of Michigan Turner Fund, the Office of The Vice-President for Research and the Shell Foundation.

Experimentally induced life-history evolution in a natural population

David A. Reznick*, Heather Bryga* & John A. Endler†

* Department of Biology, University of California, Riverside, California 92521.
† Department of Biological Sciences, University of California, Santa Barbara, California 93106, USA

LIFE-HISTORY theory predicts that reduced adult survival will select for earlier maturation and increased reproductive effort; conversely, reduced juvenile survival will select the opposite[1–5]. This is supported by laboratory studies[6–10] and comparative data from natural populations[11–15]. Laboratory studies may support a theory, but cannot assess its importance in natural populations, and comparative studies reveal correlations, not causation[16]. Long-term perturbation experiments on natural populations resolve both problems. Here we report the findings of a long-term study of guppies (*Poecilia reticulata*), in which the predictions of life-history theory are supported. Life-history differences among populations of guppies are closely associated with predator species with which guppies live[13,17–21]. The predators apparently alter age-specific survival because they are size-specific in their choice of prey[21–23]. *Crenicichla alta* (a cichlid), the main predator at one class of localities, preys predominantly on large, sexually mature size classes of guppies[22–24]. *Rivulus hartii* (a killifish), the main predator at another class of localities, preys predominantly on small, immature size classes. Guppies from localities with *Crenicichla* mature at an earlier age, have higher reproductive effort, and have more and smaller offspring per brood than those from localities with just *Rivulus*. These differences are heritable, and correspond with theoretical predictions[17–19]. To prove that predation caused this pattern, we perturbed a natural population of guppies by changing predation against adults to predation against juveniles. This resulted in significant life-history evolution in the predicted direction after 11 years, or 30–60 generations.

In 1976, guppies were transplanted from a site on the Aripo River (Trinidad) with *C. alta* (control site) to a tributary of the Aripo which previously contained *R. hartii* but no guppies (introduction site)[24]. This manipulation released guppies from selective predation on adults and exposed them to selective predation on juveniles. This treatment should favour guppies with delayed maturity and decreased reproductive effort, compared to the control site. The founding population size was 200 adults[24], consisting of equal proportions of males and non-virgin females. As guppies have sperm storage and multiple mating, the effective founding population size was almost certainly greater than 200; founder effects are therefore unlikely. In all

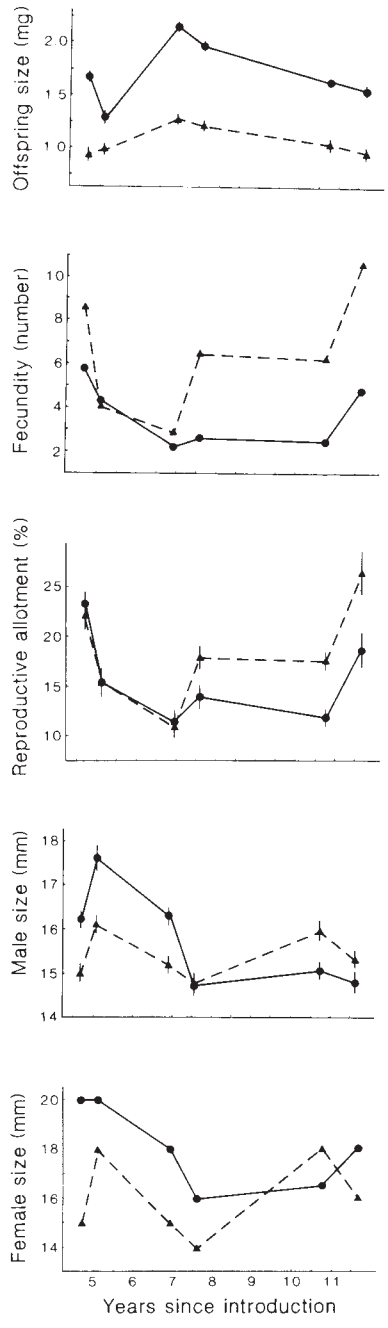

FIG. 1 Life-history phenotypes of guppies from the introduction and control sites. These data are based on wild-caught, field preserved fish. Offspring Size, mean dry weight of developing embryos, corrected for their stage of development and female size. Fecundity, expected number of offspring for a 30 mg (somatic dry weight) female. Reproductive Allotment, per cent of total dry weight that consists of developing embryos, and is corrected for the stage of development of the embryos. Male Size, average size of sexually mature males. Female Size, minimum mm size class in which the majority of females were carrying developing embryos. ●, Introduction site. ▲, Downstream control. All values are least-square means and one standard error from analyses of variance. All statistical comparisons were made within a collection and were executed with the SAS GLM procedure[31].